

Ice sheet modelling
of the last interglacial
period

A. Quiquet et al.

Title Page

Abstract

Introduction

Conclusions

References

Tables

Figures

◀

▶

◀

▶

Back

Close

Full Screen / Esc

Printer-friendly Version

Interactive Discussion



Contribution of Greenland ice sheet melting to sea level rise during the last interglacial period: an approach combining ice sheet modelling and proxy data

A. Quiquet¹, C. Ritz¹, H. J. Punge², and D. Salas y Mélia³

¹UJF – Grenoble 1/CNRS, Laboratoire de Glaciologie et Géophysique de l'Environnement (LGGE), UMR5183, Grenoble, 38041, France

²Laboratoire des Sciences du Climat et de l'Environnement (LSCE)/IPSL, CEA-CNRS-UVSQ, UMR8212, 91191 Gif-sur-Yvette, France

³CNRM-GAME, URA CNRS-Météo-France 1357, Toulouse, France

Received: 31 July 2012 – Accepted: 31 July 2012 – Published: 10 August 2012

Correspondence to: A. Quiquet (Aurelien.Quiquet@lgge.obs.ujf-grenoble.fr)

Published by Copernicus Publications on behalf of the European Geosciences Union.

Abstract

In the context of global warming, the contribution of the two major ice sheets, Antarctica and Greenland, to global sea level rise is a subject of key importance for the scientific community (4th assessment report of the Intergovernmental Panel on climate change, IPCC-AR4, Meehl et al., 2007). By the end of the next century, a 3–5 °C warm up is expected in Greenland. Similar temperatures in this region were reached during the last interglacial (LIG) period due to a change in orbital configuration rather than to anthropogenic forcing. Ice core evidence suggests that the Greenland Ice Sheet (GIS) has survived this warm period but great uncertainties remain about the total Greenland ice reduction during the LIG and its sea level rise contribution. In order to improve our confidence in future state projections, we first intend to reconstruct the past states of the GIS using ice sheet modelling, and confront the simulations with paleo data. The chosen methodology of paleoclimate reconstruction is strongly based on proxy data. Proxy data are also used to constrain the ice sheet model during the calibration phase. Our estimates of Greenland melting contribution to sea level rise during the LIG period range from 0.65 to 1.5 m of sea level equivalent.

1 Introduction

The LIG sea level anomaly from present day stands for the highest in the last 200 ka (Vezina et al., 1999), with a likely value greater than 6.7 m (Kopp et al., 2009). However, the total Greenland ice reduction during the LIG period and its contribution to sea level rise remain largely uncertain.

Evidence about the extent and volume of the GIS during the LIG period is relatively limited. This period corresponds to the deepest part of Greenland ice cores where the signal is perturbed because of layer mixing, past surface-melting and/or basal melting. The interpretation of the Greenlandic ice cores during this period is thus often difficult. However, LIG ice is assumed to have been found at the six deep ice core drilling

CPD

8, 3345–3377, 2012

Ice sheet modelling of the last interglacial period

A. Quiquet et al.

Title Page

Abstract

Introduction

Conclusions

References

Tables

Figures

◀

▶

◀

▶

Back

Close

Full Screen / Esc

Printer-friendly Version

Interactive Discussion



sites (GRIP, GISP 2, North GRIP, Camp Century, Dye 3 and the latest one, NEEM), suggesting a fairly limited ice reduction. Pollen and sediment studies can also bring valuable information. In particular, it is very likely that the southern GIS retreated further during the LIG than during the Holocene (Vernal and Hillaire-Marcel, 2008; Colville et al., 2011). The southern GIS was however not completely deglaciated (Colville et al., 2011).

To date, few studies have been carried out to reconstruct LIG Greenland geometry with ice sheet models (ISMs). The reconstruction of past surface mass balance (SMB) in such studies is one of the major issues. The most common approach, has been to drive the model with a proxy for surface air temperature (we will refer to this formulation as the “index method”). This is the approach followed by Cuffey and Marshall (2000); Huybrechts (2002); Tarasov and Peltier (2003); Lhomme et al. (2005). Amongst these, considerable uncertainties about the estimates of GIS melting contribution to global sea level remain, ranging from 2.7 m to 5.5 m. A very few other studies have tackled the problem with a more physically based SMB. To reconstruct the GIS during the LIG period, Otto-Bliesner et al. (2006) use a one-way coupling of a General Circulation Model (GCM) with an ISM, however without any feedback of the ISM on the GCM. Robinson et al. (2011) apply a regional energy-balance moisture orographic model, driven by a climate model of intermediate complexity, to force an ISM over the last glacial-interglacial cycle. The estimates of mean sea level rise contribution differ largely in these two studies, with 2.2 to 3.4 m for Otto-Bliesner et al. (2006) and 3.7–4.4 m for Robinson et al. (2011). Table 1 lists the various previous estimates.

In the present study, we use the thermomechanically coupled ice sheet model GRISLI in order to investigate scenarios of GIS reconstructions during the LIG period. This study is the first application of a hybrid model, mixing Shallow Ice and Shallow Shelf Approximations (SIA/SSA), to reconstruct the LIG geometry of the GIS. We expect a hybrid model to reproduce the ice streams pattern better than SIA-only models. We also implemented the index method mentioned above. Compared with previous works, we however improved the formulation with a self-consistent index more

Ice sheet modelling of the last interglacial period

A. Quiquet et al.

Title Page

Abstract

Introduction

Conclusions

References

Tables

Figures



Back

Close

Full Screen / Esc

Printer-friendly Version

Interactive Discussion



representative of Greenlandic surface air temperatures. When working with proxy data, we do account for past surface elevation changes of the GIS by applying a correction. We also improve on the classical index formulation by introducing outputs from GCM simulations during the LIG. Another improvement was to re-implement a tracer transport model (Lhomme et al., 2005) to tie our reconstruction to ice core information. This tracking-particles tool was extensively used during the calibration procedure.

In Sect. 2 we first describe briefly the ISM used. The mass balance model formulation, and in particular the index method is presented in depth. In this section, we also describe our model calibration method. Section 3 is focused on the LIG reconstruction. We examine the validity of our results with regards to proxy information and sensitivity experiments.

2 Model description and set up

2.1 The GRISLI ice sheet model

GRISLI (GRenoble Ice Shelf and Land Ice model) simulates ice sheet geometry and physical properties as a function of time. Given a specific climatic forcing, the large-scale dynamic evolution is computed. This ISM is three-dimensional and thermo-mechanically coupled. It accounts for the two major flow regimes observed in large-scale ice sheets: slowly moving ice is computed following Hutter (1983) (Shallow Ice Approximation, SIA), while fast ice streams and ice shelves are computed following the MacAyeal (1989) formulation (Shallow Shelf Approximation, SSA). This model is particularly adapted for paleo-reconstruction of ice sheets because of the ice shelves component. During glacial times, this feature of GRISLI facilitates the advance onto the continental shelf. The grounding line position is thus subject to great variations. In addition, the SSA scheme is expected to provide better estimates of ice slopes at the margin of the ice sheet, whereas SIA models generally produce unrealistically high slopes. This can have an impact on the extent of the ablation zone.

Ice sheet modelling of the last interglacial period

A. Quiquet et al.

Title Page

Abstract

Introduction

Conclusions

References

Tables

Figures



Back

Close

Full Screen / Esc

Printer-friendly Version

Interactive Discussion



Paleo applications such as these have already been performed by Ritz et al. (2001); Philippon et al. (2006); Álvarez-Solas et al. (2011a) for the Antarctic ice sheet and by Peyaud et al. (2007); Álvarez-Solas et al. (2011b) for the northern hemisphere ice sheets. The more recent version of the model used here has already been the subject of a sensitivity study to atmospheric forcing fields (Quiquet et al., 2012).

The technical characteristics of GRISLI were largely discussed in the previously mentioned studies and we only describe here the most relevant features. The distinction between the three types of flow is the following:

- Ice shelves are based on a flotation criteria. Calving is assumed to happen when ice reaches a minimum critical height.
- Ice streams (dragging ice shelves) strictly correspond to the location of bedrock valleys on a specified map. This map was already used in Quiquet et al. (2012). It remains constant over the whole transient simulation and represents locations where ice streams are allowed. Then, ice streams are activated when the temperature at the ice-bed interface reaches the melting point. SSA is then used as a sliding law, as proposed by Bueler and Brown (2009). We assume a linear viscous sediment type, with a basal drag proportional to basal velocity, with a coefficient β .
- Ice velocity is computed with the SIA equations only if the considered grid point is outside the prescribed ice stream map or if the temperature at the ice-bed interface is not warm enough.

In the most recent version of the model, we re-implemented a tracer transport model (Lhomme et al., 2005). The advection problem is solved with a semi-Lagrangian formulation. Location and timing of deposition is computed on each grid point of the ISM. Depositional conditions, such as surface temperature, surface mass balance and surface elevation, are thus available for each vertical grid point within the ISM. A direct comparison with observed ice cores profiles is thus possible. In the present work, we mainly use this scheme in order to calibrate the ISM.

Ice sheet modelling of the last interglacial period

A. Quiquet et al.

Title Page

Abstract

Introduction

Conclusions

References

Tables

Figures



Back

Close

Full Screen / Esc

Printer-friendly Version

Interactive Discussion



The ISM is run here on a 15-kilometer Cartesian grid, with 21 vertical points within the ice. Bedrock data set is extracted from Amante and Eakins (2009) and re-gridded in a stereographic projection with standard parallel at 71° N and central meridian at 39° W.

Initial ice thickness is provided by Bamber et al. (2001). We use geothermal heat flux from Shapiro and Ritzwoller (2004), modified nearby ice core locations, to take into account the values derived from measured temperature depth profiles: very high value at North GRIP (Dahl-Jensen et al., 2003), and very low at Dye 3 (Dahl-Jensen et al., 1998).

2.2 The surface mass balance model

2.2.1 The standard index method

We use an index method to reconstruct past surface mass balance (SMB). In this approach, present day atmospheric temperature is perturbed by a spatially uniform anomaly of temperature deduced from proxy data. As mentioned earlier, this method has already been widely used for GIS paleo reconstructions (Letréguilly et al., 1991; Ritz et al., 1997; Greve, 1997; Cuffey and Marshall, 2000; Huybrechts, 2002; Tarasov and Peltier, 2003; Lhomme et al., 2005) and within the EISMINT (European Ice Sheet Modelling INiTiative) framework (Huybrechts et al., 1996).

The first reason why we chose this formulation is because it relies on a very small number of tunable parameters. Considering the large discrepancies in present day SMB simulations between atmospheric models (Yoshimori and Abe-Ouchi, 2012), we may have similar uncertainties regarding the LIG SMB. The index method can be easily tuned to reproduce present day GIS topography and data derived from ice cores studies. The second reason is because it relies strongly on proxy data, which are strong constraints for past climatic conditions.

Present day atmospheric conditions (namely monthly near surface air temperature and total precipitation) are deduced from outputs of two Regional Circulation Models (RCMs). We used the RACMO2 (Ettema et al., 2009) and the MAR (Fettweis et al.,

Ice sheet modelling of the last interglacial period

A. Quiquet et al.

Title Page

Abstract

Introduction

Conclusions

References

Tables

Figures



Back

Close

Full Screen / Esc

Printer-friendly Version

Interactive Discussion



2011) models, averaged over the 1958–2007 period. We developed a composite map of these two RCMs in order to have a good agreement between simulated present day accumulation rates and measured accumulation rates at the five GIS deep ice core sites (Dye 3, GRIP, North GRIP, NEEM, Camp Century).

5 A time dependent but spatially uniform perturbation, $\Delta T_s|_{(t)}$, is superimposed onto the present day near surface air temperature field, $T_s^{\text{pd}}|_{(x,y)}$, in order to evaluate the past near surface air temperature field:

$$T_s|_{(t,x,y)} = T_s^{\text{pd}}|_{(x,y)} + \Delta T_s|_{(t)} \quad (1)$$

This perturbation in surface temperature is deduced from proxy data of climate.

10 The most common proxy used is isotopic content in $\delta^{18}\text{O}$ at GRIP or North GRIP. As mentioned earlier, in previous studies, the $\delta^{18}\text{O}$ proxy was completed by the deuterium record for ages older than the LIG period (e.g. Cuffey and Marshall, 2000; Huybrechts, 2002; Lhomme et al., 2005). Section 2.2.2 deals with our choice of proxy for temperature.

15 In any case, the $\delta^{18}\text{O}$ proxy is converted into temperature anomaly with the relation:

$$\delta^{18}\text{O}|_{(t)} = \alpha^i \Delta T_s|_{(t)} \quad (2)$$

The α^i coefficient, hereafter called the isotopic slope, is relatively unconstrained. The value of this slope is generally inferred while comparing simulated and measured temperature profile at ice core drilling sites. This calibration is however ice model-
20 dependent. In particular, the simulated temperature profile is strongly dependent of past evolution of ice margins (e.g. Cuffey and Clow, 1997).

We assume a spatially uniform lapse rate to take into account the feedback of surface elevation changes on temperature. This lapse rate is assumed to have seasonal variations, being lower in summer than in winter. Monthly values however remain constant
25 over the transient simulation.

Temperature changes affect the precipitation rate and the following correction is done, with $P_r^{\text{pd}}|_{(x,y)}$, the present day total precipitation rate, and $P_r|_{(t,x,y)}$, the past total

Ice sheet modelling of the last interglacial period

A. Quiquet et al.

Title Page

Abstract

Introduction

Conclusions

References

Tables

Figures



Back

Close

Full Screen / Esc

Printer-friendly Version

Interactive Discussion



precipitation rate:

$$P_r|_{(t,x,y)} = P_r^{\text{pd}}|_{(x,y)} \exp \left(-\gamma \left(T_s|_{(t,x,y)} - T_s^{\text{pd}}|_{(x,y)} \right) \right) \quad (3)$$

In our approach, ablation is computed with a Positive Degree Day (PDD) formulation (Reeh, 1991). PDDs are calculated with the monthly means of near surface temperature. PDD coefficients follow Tarasov and Peltier (2002). We make a distinction between solid and liquid precipitation following Marsiat (1994). We take into account that melt water and rainfall may refreeze in the firn layer, using a parameterization adapted from Janssens and Huybrechts (2000).

We are aware that we are using a rather simplified approach and that some important processes might be missing, such as the LIG insolation anomaly compared with present day (Berg et al., 2011) and its role in the ablation rate. However, even the most sophisticated RCMs disagree in simulating the present day SMB of the ice sheet. We prefer to adopt a simpler approach that is nonetheless more connected to proxy information.

2.2.2 A multi-proxy index for near surface air temperature

The index method relies on temperature perturbations. The last interglacial period should of course be covered by this index, as well as several tens of thousands of years prior to this period in order to take into account the previous glacial stage and its effect on the ice sheet response.

The value of $\delta^{18}\text{O}$ measured in Greenland ice cores (North GRIP members, 2004) is generally used as a proxy for temperature in this region. However, up to now, none of the Greenland ice cores shows a continuous measurement of $\delta^{18}\text{O}$ reaching back to a period in time older than 123 ka. Alternatives have to be found to reconstruct past surface air temperature over this period of time.

Past studies with a similar approach to ours have mainly used a composite index with a combination of GRIP $\delta^{18}\text{O}$ and Vostok deuterium excess (Cuffey and Marshall, 2000; Huybrechts, 2002; Lhomme et al., 2005). However, ice cores show asynchronous

Ice sheet modelling of the last interglacial period

A. Quiquet et al.

Title Page

Abstract

Introduction

Conclusions

References

Tables

Figures

◀

▶

◀

▶

Back

Close

Full Screen / Esc

Printer-friendly Version

Interactive Discussion



climatic signals between the two hemispheres (e.g. Blunier et al., 1998). The use of the Vostok core to construct a temperature history for Greenland is a drastic simplification leading to large errors in timing as well as in amplitude.

In order to improve on that, we search for proxy directly linked with North hemisphere temperature or at least global.

Considering its relatively high mixing ratio, methane is considered as a relatively robust indicator of past climate, in particular temperature, at the millennial timescale (Loulergue et al., 2008). We use here the EPICA DOME-C methane concentration measurements (Lüthi et al., 2008; Loulergue et al., 2008). We scaled the methane amplitude to the NGRIP $\delta^{18}O$ for the first 123 ka in order to have a reasonable temperature variability prior to the last interglacial period. A direct calibration between Greenland temperature (via $\delta^{18}O$) and methane concentration is still a strong simplification. $\delta^{18}O$ may be more representative of the winter temperature (Denton et al., 2005) while methane is a proxy for global annual mean temperature. Moreover, it seems that the maximum in methane concentration (around 128 ka) came several thousand years earlier than the supposed maximum Greenland temperature (Masson-Delmotte et al., 2010). In order to have a better estimate of the LIG timing, we chose a Sea Surface Temperature (SST) reconstruction from the ODP980 North Atlantic marine core (McManus et al., 1999; Oppo et al., 2006). Here again, we scaled the SST amplitude to the $\delta^{18}O$ when the two signals overlap. We took special care to have all our proxies on the same timescale, being the one of Lemieux-Dudon et al. (2010). A comparison between these proxies around the LIG period is shown in Fig. 1. An additional improvement over previous works is that we corrected the measured NGRIP $\delta^{18}O$ to take into account past surface elevation change. Isotopic values measured along the ice cores are indeed modulated by surface elevation changes, but the index must be representative of a temperature anomaly for a constant surface elevation. Both scaling of methane and SST to the NGRIP $\delta^{18}O$ has been done only after this surface elevation correction.

The multi-proxy index obtained, expressed in terms of $\delta^{18}O$, is finally converted into temperature assuming a simple linear relationship. The multi-proxy index obtained is

Ice sheet modelling of the last interglacial period

A. Quiquet et al.

Title Page

Abstract

Introduction

Conclusions

References

Tables

Figures



Back

Close

Full Screen / Esc

Printer-friendly Version

Interactive Discussion



shown in Fig. 2. The temperature perturbation used in this study is available in the Supplement.

2.2.3 Introduction of GCM simulations in the index method

The direct perturbation of present day atmospheric fields with the previously described index does not account for changes in atmospheric circulation and the consequences on temperature and precipitation. To improve on that, we also used GCM snapshots run at 126 ka with the present day topography of the GIS but with a 126 ka orbital forcing and greenhouse gases. The two GCMs used were selected among the CMIP-3 models for their availability over the LIG period:

- the IPSL-CM4 (Marti et al., 2010; Braconnot et al., 2008)
- the CNRM-CM3.3 (Salas-Mélia et al., 2005)

Quiquet et al. (2012) have shown that an anomaly method (“best” present day climatology + perturbation deduced from GCMs) is preferable to a direct forcing with absolute fields from coarse resolution GCMs. To account for this we use, at each ISM grid point (x, y) , GCM anomalies at 126 BP, $T_s^{\text{GCM}}|_{(126,x,y)} - T_s^{\text{GCM}}|_{(0,x,y)}$, on top of present day forcing fields:

$$\begin{cases} T_s|_{(126,x,y)} = T_s^{\text{pd}}|_{(x,y)} + (T_s^{\text{GCM}}|_{(126,x,y)} - T_s^{\text{GCM}}|_{(0,x,y)}) \\ P_r|_{(126,x,y)} = P_r^{\text{pd}}|_{(x,y)} + (P_r^{\text{GCM}}|_{(126,x,y)} - P_r^{\text{GCM}}|_{(0,x,y)}) \end{cases} \quad (4)$$

The obtained snapshot at 126 kyrs is then here again perturbed with an index. The previously prescribed index was designed to present a zero-anomaly at 0 ka BP and has to be modified for use with the anomaly method in order to present a zero-anomaly at 126 ky BP.

In the following, we will refer to the “no-anomaly experiment” for the direct application of the index on present day forcing field and respectively to “CNRM and ISPL anomaly experiment” for the two others.

Ice sheet modelling of the last interglacial period

A. Quiquet et al.

Title Page

Abstract

Introduction

Conclusions

References

Tables

Figures

⏪

⏩

◀

▶

Back

Close

Full Screen / Esc

Printer-friendly Version

Interactive Discussion



2.3 Model calibration

To calibrate the ISM we run transient experiments for the last 60 ka BP. We selected the parameters of the model in order to be as close as possible to the present day state of the GIS. For that, we used the following constraints:

- Simulated geometry as close as possible to the one of Bamber et al. (2001).
- Simulated surface velocity field close to the present day observations of Joughin et al. (2010).

In addition to these large scale features, we also included constraints from ice core drilling:

- Simulated temperature profile similar to the borehole measurements.
- Simulated age-depth relationship close to the GICC05 timescale (Rasmussen et al., 2006).

We owe the possibility of using an age-depth relationship as a constraint to the newly re-implemented tracer transport model. The simulated age-depth relationship at ice core locations is compared with the GICC05 timescale in Fig. 3.

The simulated geometry of the GIS is mainly driven by SMB and dynamical parameters of the ISM, in particular the ice extent is governed by the choice of ablation coefficients of the PDD method and modulated by the choice of dynamical parameters. On the other hand, the temperature profile and age-depth relationship mainly depend on the paleo-perturbation, such as the glacial-interglacial amplitude of temperature change and precipitation ratio given by Eq. (3).

Our choice of parameters is summarized in Table 2. The present day precipitation rate was extracted from a combination of two RCMs, the RACMO (Ettema et al., 2009) and MAR (Fettweis et al., 2011) models. The combination was done in order to have a better agreement between the observed accumulation rate at ice cores locations

Ice sheet modelling of the last interglacial period

A. Quiquet et al.

Title Page

Abstract

Introduction

Conclusions

References

Tables

Figures



Back

Close

Full Screen / Esc

Printer-friendly Version

Interactive Discussion



and the one derived from the forcing field. This agreement is necessary to compare age-depth relationships. Present day near surface temperature field for the present study is the one prescribed from the EISMINT experiments (Huybrechts et al., 1996) where temperature is a simple function of latitude and elevation. We have selected this present temperature parameterisation because it fits better the observed present surface temperature at the drilling sites, a condition necessary to reproduce the observed temperature profiles. The geothermal heat flux from Shapiro and Ritzwoller (2004) was locally modified in particular to take into account the measured large anomaly at North GRIP and low anomaly at Dye 3.

The present day simulated geometry of the GIS after calibration is compared with observations in Fig. 4.

3 Results

3.1 Simulated topographies and sea level contribution

We performed transient simulations of the last 200 ka with the calibrated version of the model. Figure 5 presents the simulated contribution of Greenland melting to sea level rise over the last glacial-interglacial cycle. The minimum in ice volume is achieved at around 121 ka BP in our reconstructions. The GIS geometry at this time is represented in Fig. 6 for the three experiments described previously (no-anomaly, CNRM and IPSL anomalies). The pattern of retreat is relatively similar in the 3 experiments: the northeastern and southwestern margins retreat more than the other regions. Ice is preserved at ice core locations in all three experiments and the South dome is relatively stable, which is compatible with geological evidence (Colville et al., 2011).

It clearly appears that the no-anomaly experiment has the most retreating GIS. It can be explained by the difference in surface temperature imposed during LIG. At North GRIP, the two GCMs present a 126 ka BP annual mean near surface temperature very similar to the present day value. In contrast, the index presented in Fig. 2 exhibits a

Ice sheet modelling of the last interglacial period

A. Quiquet et al.

Title Page

Abstract

Introduction

Conclusions

References

Tables

Figures



Back

Close

Full Screen / Esc

Printer-friendly Version

Interactive Discussion



+5 °C 126 ka BP annual mean near surface temperature anomaly. This difference is however smaller in summer. The mean July temperature anomaly at North GRIP in the IPSL model is also +5 °C, which is equivalent to the index. CNRM is however somewhat colder at North GRIP with only a +3 °C anomaly in July temperature.

We raise here one of the major questions concerning the index method: is the isotopic content representative for annual or summer temperature? Considering one or the other option will locally introduce some bias depending on the geographical position and also the time considered.

In all our simulations, ice is preserved at each ice core location. Changes in elevation are however drastic in the no-anomaly experiment for the sites of Dye 3, Camp Century and NEEM.

Our estimates of the GIS melting contribution to mean sea level rise during the LIG period are as follows:

- No-anomaly experiment: 2.90–3.71 m.
- CNRM anomaly experiment: 0.65–1.46 m.
- IPSL anomaly experiment: 0.68–1.50 m.

The lower bound of these estimate corresponds to the difference between the LIG minimum volume simulated by the ISM and the observed present day volume. The upper bound represents the difference between the same LIG volume and the simulated present day volume. Thus, the upper bound takes into account the ISM bias in simulating ice retreat, because of an overestimation of simulated present day volume by 10–15%. We wish to stress that the calibration was not done only on the volume, but also on the extent, the velocity field and on deep ice core drilling information in terms of temperature profile and age-depth relationship. We think that the resulting set of parameters is more robust than the one we would have obtained with a volume calibration alone.

The ranges of simulated volume for the two experiments with anomalies are very similar. Taking into account the changes in atmospheric circulation seems to decrease the

Ice sheet modelling of the last interglacial period

A. Quiquet et al.

Title Page

Abstract

Introduction

Conclusions

References

Tables

Figures



Back

Close

Full Screen / Esc

Printer-friendly Version

Interactive Discussion



sensitivity of the GIS to the LIG warming. However, further studies should repeat these experiments with more GCMs in order to increase our confidence in this result. The different representations of physical and dynamic processes among GCMs may lead to different sensitivities to solar parameter-induced warming. The difference between the no-anomaly experiment and the two others may also reflect the inability of GCMs to reproduce the highly variable paleo climate (e.g. Masson-Delmotte et al., 2006). In addition, these GCM simulations do not take GHG variations into account, but simply assume fixed pre-industrial conditions. A complete carbon cycle model would be needed. GCMs often suffer also from simplified snow representations. For example, no albedo changes is assumed for Eemian vs pre-industrial, although these may have a significant impact and increase the LIG temperature anomaly (e.g. Punge et al., 2012).

The robustness of our results to the choice of parameters was briefly tested in sensitivity experiments. In particular, the accumulation ratio γ , and the isotopic slope α^i , have an important effect on past climate reconstruction assumptions that are likely to affect the simulated ice sheet. Figure 8 shows that the two experiments using GCM anomalies are relatively robust. On the contrary, the precipitation ratio seems to greatly affect the results in the no-anomaly experiment. The value of 0.05°C leading to an almost complete melting of the GIS.

3.2 Paleo data confrontation: is the warming realistic?

Our reconstructions depend mainly on our climatic assumptions. In particular, the chosen index governs the near surface air temperature amplitude change over the GIS.

Some reconstructions of the possible range of temperature change based on proxy estimates are however available. The estimated range of summer near surface temperature in Greenland based on various proxy is $4\text{--}5^\circ\text{C}$ (Members, 2006).

Figure 7 shows the evolution of July near surface temperature at ice core locations. Note that in our PDD formulation, melt is possible with surface temperatures greater than -5°C . With this condition, the sites of Dye 3, Camp Century and even NEEM are

CPD

8, 3345–3377, 2012

Ice sheet modelling of the last interglacial period

A. Quiquet et al.

Title Page

Abstract

Introduction

Conclusions

References

Tables

Figures

⏪

⏩

◀

▶

Back

Close

Full Screen / Esc

Printer-friendly Version

Interactive Discussion



affected by summer melting in all of our three experiments. If our estimates are correct, the NEEM ice core should show evidence of melting.

The July near surface air temperature presented in Fig. 7 accounts for surface elevation changes. The no-anomaly experiment produces a change in surface elevation greater than one thousand metres at Camp Century, and results in a drastic July temperature increase (more than +12°C compared with the present day value). There is indeed no evidence in ice cores of such a great surface elevation change at Camp Century. We therefore consider our no-anomaly experiment to be probably not realistic.

For the two GCM anomaly experiments, the LIG warming compared with present day was higher at North GRIP than in Camp Century due to surface elevation changes. LIG surface elevation at North GRIP was slightly lower, while higher at Camp Century. At North GRIP, we have a +4°C (CNRM) and +6°C (IPSL) increase whereas the increase is only +2°C at Camp Century for both experiments. This range is however compatible with what is estimated from proxy (Members, 2006).

4 Conclusions

Based on this study, we provide estimations, strongly based on proxy information, of the possible GIS melting contribution to sea level rise during the LIG, using a hybrid ice sheet model. South Dome is relatively stable even in a warm climate, while the northernmost ice core locations seem to be the ones at risk. We presented three different experiments. The no-anomaly experiment results in great variations of surface elevation in particular at the margin. Given that ice cores show no evidence of such drastic changes, we consider this reconstruction to be unrealistic. Keeping only the two experiments with GCM anomalies, we suggest a GIS melting contribution to sea level rise ranging from 0.65 to 1.50 m with a preferred estimate of approximately 1 m. This low value suggests a large contribution from the Antarctic ice sheet.

The reconstructions presented here are however tainted by the simplifications required to achieve them. We have shown that reconstructions are highly sensitive to

Ice sheet modelling of the last interglacial period

A. Quiquet et al.

Title Page

Abstract

Introduction

Conclusions

References

Tables

Figures



Back

Close

Full Screen / Esc

Printer-friendly Version

Interactive Discussion



changes in atmospheric circulation. One way to improve confidence in our reconstructions would be to include more temporal snapshots. Another way would be to increase the number of GCMs used. There are still only few GCM simulations of the LIG but they are becoming available. One of the major simplifications of the index method is the use of a simple lapse rate to take into account the impact of surface elevation changes on temperature. To improve on that, further studies should include GCM simulations with various topographies of the GIS during the LIG.

A direct coupling of a GCM with an ISM (at least a oneway coupling) would be more realistic in an idealised representation but would also be strongly dependent on the GCM used, as mentioned in Quiquet et al. (2012). Another disadvantage of a direct coupling is the apparent inability of GCMs to reproduce the high variability observed in proxy data. Incorporating proxy constraints into GCMs is required (Masson-Delmotte et al., 2006) to obtain more accurate results.

Supplementary material related to this article is available online at:

<http://www.clim-past-discuss.net/8/3345/2012/cpd-8-3345-2012-supplement.pdf>.

Acknowledgements. We thank CISM for providing the datasets of Shapiro and Ritzwoller (2004) and Joughin et al. (2010). Janneke Ettema, Jan van Angelen and Michiel van den Broeke (IMAU, Utrecht University) are thanked for providing RACMO2 climate fields, Xavier Fettweiss for providing the MAR climate fields and Pascale Braconnot for providing the IPSL LIG runs. Aurélien Quiquet is supported by the ANR project NEEM-France and European commission FP7 project PAST4FUTURE. NEEM is directed and organized by the Center of Ice and Climate at the Niels Bohr Institute and US NSF, Office of Polar Programs. It is supported by funding agencies and institutions in Belgium (FNRS-CFB and FWO), Canada (NRCan/GSC), China (CAS), Denmark (FIST), France (IPEV, CNRS/INSU, CEA and ANR), Germany (AWI), Iceland (RannIs), Japan (NIPR), Korea (KOPRI), The Netherlands (NWO/ALW), Sweden (VR),

Ice sheet modelling of the last interglacial period

A. Quiquet et al.

Title Page

Abstract

Introduction

Conclusions

References

Tables

Figures



Back

Close

Full Screen / Esc

Printer-friendly Version

Interactive Discussion



Switzerland (SNF), UK (NERC) and the USA (US NSF, Office of Polar Programs). This is Past4Future contribution no. 29. The research leading to these results has received funding from the European Union's Seventh Framework programme (FP7/2007-2013) under grant agreement no 243908, "Past4Future. Climate change – Learning from the past climate". All (or most of) the computations presented in this paper were performed using the CIMENT infrastructure (<https://ciment.ujf-grenoble.fr>), which is supported by the Rhône-Alpes region (GRANT CPER07_13 CIRA: <http://www.ci-ra.org>).



The publication of this article is financed by CNRS-INSU.

References

- Álvarez-Solas, J., Charbit, S., Ramstein, G., Paillard, D., Dumas, C., Ritz, C., and Roche, D. M.: Millennial-scale oscillations in the Southern Ocean in response to atmospheric CO₂ increase, *Global Planet. Change*, 76, 128–136, 2011a. 3349
- Álvarez-Solas, J., Montoya, M., Ritz, C., Ramstein, G., Charbit, S., Dumas, C., Nisancioglu, K., Dokken, T., and Ganopolski, A.: Heinrich event 1: an example of dynamical ice-sheet reaction to oceanic changes, *Clim. Past*, 7, 1297–1306, doi:10.5194/cp-7-1297-2011, 2011b. 3349
- Amante, C. and Eakins, B.: ETOPO1 1 Arc-Minute Global Relief Model: Procedures, Data Sources and Analysis, NOAA Technical Memorandum NESDIS NGDC-24, 19 pp., 2009. 3350
- Bamber, J. L., Layberry, R. L., and Gogineni, S. P.: A new ice thickness and bed data set for the Greenland ice sheet 1. Measurement, data reduction, and errors, *J. Geophys. Res.*, 106, 33773–33780, doi:10.1029/2001JD900054, 2001. 3350, 3355, 3373

Ice sheet modelling of the last interglacial period

A. Quiquet et al.

Title Page

Abstract

Introduction

Conclusions

References

Tables

Figures



Back

Close

Full Screen / Esc

Printer-friendly Version

Interactive Discussion



Ice sheet modelling of the last interglacial period

A. Quiquet et al.

Title Page

Abstract

Introduction

Conclusions

References

Tables

Figures

◀

▶

◀

▶

Back

Close

Full Screen / Esc

Printer-friendly Version

Interactive Discussion



- Berg, W. J. v. d., Broeke, M. v. d., Ettema, J., Meijgaard, E. v., and Kaspar, F.: Significant contribution of insolation to Eemian melting of the Greenland ice sheet, *Nat. Geosci.*, 4, 679–683, doi:10.1038/ngeo1245, 2011. 3352
- Blunier, T., Chappellaz, J., Schwander, J., Dällenbach, A., Stauffer, B., Stocker, T. F., Raynaud, D., Jouzel, J., Clausen, H. B., Hammer, C. U., and Johnsen, S. J.: Asynchrony of Antarctic and Greenland climate change during the last glacial period, *Nature*, 394, 739–743, doi:10.1038/29447, 1998. 3353
- Braconnot, P., Marzin, C., Grégoire, L., Mosquet, E., and Marti, O.: Monsoon response to changes in Earth's orbital parameters: comparisons between simulations of the Eemian and of the Holocene, *Clim. Past*, 4, 281–294, doi:10.5194/cp-4-281-2008, 2008. 3354
- Bueler, E. and Brown, J.: Shallow shelf approximation as a “sliding law” in a thermomechanically coupled ice sheet model, *J. Geophys. Res.*, 114, F3008, doi:10.1029/2008JF001179, 2009. 3349
- Colville, E. J., Carlson, A. E., Beard, B. L., Hatfield, R. G., Stoner, J. S., Reyes, A. V., and Ullman, D. J.: Sr-Nd-Pb Isotope Evidence for Ice-Sheet Presence on Southern Greenland During the Last Interglacial, *Science*, 333, 620–623, doi:10.1126/science.1204673, 2011. 3347, 3356
- Cuffey, K. M. and Clow, G. D.: Temperature, accumulation, and ice sheet elevation in central Greenland through the last deglacial transition, *J. Geophys. Res.*, 102, 26383–26396, 1997. 3351
- Cuffey, K. M. and Marshall, S. J.: Substantial contribution to sea-level rise during the last interglacial from the Greenland ice sheet, *Nature*, 404, 591–594, 2000. 3347, 3350, 3351, 3352, 3368
- Dahl-Jensen, D., Mosegaard, K., Gundestrup, N., Clow, G. D., Johnsen, S. J., Hansen, A. W., and Balling, N.: Past Temperatures Directly from the Greenland Ice Sheet, *Science*, 282, 268–271, doi:10.1126/science.282.5387.268, 1998. 3350
- Dahl-Jensen, D., Gundestrup, N., Gogineni, S. P., and Miller, H.: Basal melt at NorthGRIP modeled from borehole, ice-core and radio-echo sounder observations, *Ann. Glaciol.*, 37, 207–212, doi:10.3189/172756403781815492, 2003. 3350
- Denton, G. H., Alley, R. B., Comer, G. C., and Broecker, W. S.: The role of seasonality in abrupt climate change, *Quaternary Sci. Rev.*, 24, 1159–1182, doi:10.1016/j.quascirev.2004.12.002, 2005. 3353

Ice sheet modelling of the last interglacial period

A. Quiquet et al.

Title Page

Abstract

Introduction

Conclusions

References

Tables

Figures

◀

▶

◀

▶

Back

Close

Full Screen / Esc

Printer-friendly Version

Interactive Discussion



- Ettema, J., van den Broeke, M. R., van Meijgaard, E., van de Berg, W. J., Bamber, J. L., Box, J. E., and Bales, R. C.: Higher surface mass balance of the Greenland ice sheet revealed by high-resolution climate modeling, *Geophys. Res. Lett.*, 36, 1–5, doi:10.1029/2009GL038110, 2009. 3350, 3355
- 5 Fettweis, X., Tedesco, M., van den Broeke, M., and Ettema, J.: Melting trends over the Greenland ice sheet (1958–2009) from spaceborne microwave data and regional climate models, *The Cryosphere*, 5, 359–375, doi:10.5194/tc-5-359-2011, 2011. 3350, 3355
- Greve, R.: Application of a polythermal three-dimensional ice sheet model to the Greenland ice sheet: Response to steady-state and transient climate scenarios, *J. Climate*, 10, 901–918, doi:10.1175/1520-0442(1997)010<0901:AOAPTD>2.0.CO;2, 1997. 3350
- 10 Hutter, K.: *Theoretical glaciology: material science of ice and the mechanics of glaciers and ice sheets*, Reidel Publishing Company, Dordrecht, The Netherlands, 1983. 3348
- Huybrechts, P.: Sea-level changes at the LGM from ice-dynamic reconstructions of the Greenland and Antarctic ice sheets during the glacial cycles, *Quaternary Sci. Rev.*, 21, 203–231, doi:10.1016/S0277-3791(01)00082-8, 2002. 3347, 3350, 3351, 3352
- 15 Huybrechts, P., Payne, T., and EISMINT Intercomparison Group: The EISMINT benchmarks for testing ice-sheet models, *Ann. Glaciol.*, 23, 1–12, 1996. 3350, 3356
- Janssens, I. and Huybrechts, P.: The treatment of meltwater retardation in mass-balance parameterizations of the Greenland ice sheet, *Ann. Glaciol.*, 31, 133–140, 2000. 3352
- 20 Joughin, I., Smith, B. E., Howat, I. M., Scambos, T., and Moon, T.: Greenland flow variability from ice-sheet-wide velocity mapping, *J. Glaciol.*, 56, 415–430, doi:10.3189/002214310792447734, 2010. 3355, 3360
- Kopp, R. E., Simons, F. J., Mitrovica, J. X., Maloof, A. C., and Oppenheimer, M.: Probabilistic assessment of sea level during the last interglacial stage, *Nature*, 462, 863–867, doi:10.1038/nature08686, 2009. 3346
- 25 Lemieux-Dudon, B., Blayo, E., Petit, J., Waelbroeck, C., Svensson, A., Ritz, C., Barnola, J., Narcisi, B. M., and Parrenin, F.: Consistent dating for Antarctic and Greenland ice cores, *Quaternary Sci. Rev.*, 29, 8–20, doi:10.1016/j.quascirev.2009.11.010, 2010. 3353
- Letréguilly, A., Reeh, N., and Huybrechts, P.: The Greenland ice sheet through the last glacial-interglacial cycle, *Global Planet. Change*, 4, 385–394, doi:10.1016/0921-8181(91)90004-G, 1991. 3350
- 30

Ice sheet modelling of the last interglacial period

A. Quiquet et al.

Title Page

Abstract

Introduction

Conclusions

References

Tables

Figures

◀

▶

◀

▶

Back

Close

Full Screen / Esc

Printer-friendly Version

Interactive Discussion



- Lhomme, N., Clarke, G. K., and Marshall, S. J.: Tracer transport in the Greenland Ice Sheet: constraints on ice cores and glacial history, *Quaternary Sci. Rev.*, 24, 173–194, doi:10.1016/j.quascirev.2004.08.020, 2005. 3347, 3348, 3349, 3350, 3351, 3352, 3368
- Loulergue, L., Schilt, A., Spahni, R., Masson-Delmotte, V., Blunier, T., Lemieux, B., Barnola, J., Raynaud, D., Stocker, T. F., and Chappellaz, J.: Orbital and millennial-scale features of atmospheric CH₄ over the past 800,000 years, *Nature*, 453, 383–386, doi:10.1038/nature06950, 2008. 3353
- Lüthi, D., Le Floch, M., Bereiter, B., Blunier, T., Barnola, J., Siegenthaler, U., Raynaud, D., Jouzel, J., Fischer, H., Kawamura, K., and Stocker, T. F.: High-resolution carbon dioxide concentration record 650,000–800,000 years before present, *Nature*, 453, 379–382, doi:10.1038/nature06949, 2008. 3353
- MacAyeal, D. R.: Large-Scale Ice Flow Over a Viscous Basal Sediment: Theory and Application to Ice Stream B, Antarctica, *J. Geophys. Res.*, 94, 4071–4087, doi:10.1029/JB094iB04p04071, 1989. 3348
- Marsiat, I.: Simulation of the northern hemisphere continental ice sheets over the last glacial-interglacial cycle: experiments with a latitude-longitude vertically integrated ice sheet model coupled to zonally averaged climate model, *Paleoclimates*, 1, 59–98, 1994. 3352
- Marti, O., Braconnot, P., Dufresne, J., Bellier, J., Benshila, R., Bony, S., Brockmann, P., Cadule, P., Caubel, A., Codron, F., Noblet, N., Denvil, S., Fairhead, L., Fichefet, T., Foujols, M., Friedlingstein, P., Goosse, H., Grandpeix, J., Guilyardi, E., Hourdin, F., Idelkadi, A., Kageyama, M., Krinner, G., Lvy, C., Madec, G., Mignot, J., Musat, I., Swingedouw, D., and Talandier, C.: Key features of the IPSL ocean atmosphere model and its sensitivity to atmospheric resolution, *Clim. Dynam.*, 34, 1–26, doi:10.1007/s00382-009-0640-6, 2010. 3354
- Masson-Delmotte, V., Kageyama, M., Braconnot, P., Charbit, S., Krinner, G., Ritz, C., Guilyardi, E., Jouzel, J., Abe-Ouchi, A., Crucifix, M., Gladstone, R. M., Hewitt, C. D., Kitoh, A., LeGrande, A. N., Marti, O., Merkel, U., Motoi, T., Ohgaito, R., Otto-Bliesner, B., Peltier, W. R., Ross, I., Valdes, P. J., Vettoretti, G., Weber, S. L., Wolk, F., and Yu, Y.: Past and future polar amplification of climate change: climate model intercomparisons and ice-core constraints, *Clim. Dynam.*, 26, 513–529, doi:10.1007/s00382-005-0081-9, 2006. 3358, 3360
- Masson-Delmotte, V., Stenni, B., Blunier, T., Cattani, O., Chappellaz, J., Cheng, H., Dreyfus, G., Edwards, R. L., Falourd, S., Govin, A., Kawamura, K., Johnsen, S. J., Jouzel, J., Landais, A., Lemieux-Dudon, B., Laurantou, A., Marshall, G., Minster, B., Mudelsee, M., Pol, K.,

Ice sheet modelling of the last interglacial period

A. Quiquet et al.

Title Page

Abstract

Introduction

Conclusions

References

Tables

Figures



Back

Close

Full Screen / Esc

Printer-friendly Version

Interactive Discussion



Röthlisberger, R., Selmo, E. , and Waelbroeck, C.: Abrupt change of Antarctic moisture origin at the end of Termination II, *Proc. Natl. Acad. Sci.*, 107, 12091–12094, 2010. 3353

McManus, J. F., Oppo, D. W., and Cullen, J. L.: A 0.5-Million-Year Record of Millennial-Scale Climate Variability in the North Atlantic, *Science*, 283, 971–975, doi:10.1126/science.283.5404.971, 1999. 3353

Meehl, G. A., Stocker, T. F., Collins, W. D., Friedlingstein, P., Gaye, A. T., Gregory, J. M., Kitoh, A., Knutti, R., Murphy, J. M., Noda, A., Raper, S. C. B., Watterson, I. G., Weaver, A. J., and Zhao, Z.-C.: Global climate projections, in: *Climate Change 2007: The Physical Science Basis. Contribution of Working Group I to the Fourth Assessment Report of the Intergovernmental Panel on Climate Change*, edited by: Solomon, S., Qin, D., Manning, M., Chen, Z., Marquis, M., Averyt, K. B., Tignor, M., and Miller, H. L., Cambridge Univ. Press, 2007. 3346

Members, C.: Last Interglacial Arctic warmth confirms polar amplification of climate change, *Quaternary Sci. Rev.*, 25, 1383–1400, doi:10.1016/j.quascirev.2006.01.033, 2006. 3358, 3359

North GRIP members: High-resolution record of Northern Hemisphere climate extending into the last interglacial period, *Nature*, 431, 147–151, 2004. 3352

Oppo, D. W., McManus, J. F., and Cullen, J. L.: Evolution and demise of the Last Interglacial warmth in the subpolar North Atlantic, *Quaternary Sci. Rev.*, 25, 3268–3277, doi:10.1016/j.quascirev.2006.07.006, 2006. 3353

Otto-Bliesner, B. L., Marshall, S. J., Overpeck, J. T., Miller, G. H., and Hu, A.: Simulating Arctic Climate Warmth and Icefield Retreat in the Last Interglaciation, *Science*, 311, 1751–1753, 2006. 3347, 3368

Peyaud, V., Ritz, C., and Krinner, G.: Modelling the Early Weichselian Eurasian Ice Sheets: role of ice shelves and influence of ice-dammed lakes, *Clim. Past*, 3, 375–386, doi:10.5194/cp-3-375-2007, 2007. 3349

Philippon, G., Ramstein, G., Charbit, S., Kageyama, M., Ritz, C., and Dumas, C.: Evolution of the Antarctic ice sheet throughout the last deglaciation: A study with a new coupled climate–north and south hemisphere ice sheet model, *Earth Planet. Sci. Lett.*, 248, 750–758, doi:10.1016/j.epsl.2006.06.017, 2006. 3349

Punge, H. J., Gallée, H., Kageyama, M., and Krinner, G.: Modelling snow accumulation on Greenland in Eemian, glacial inception and modern climates in a GCM, *Clim. Past Discuss.*, 8, 1523–1565, doi:10.5194/cpd-8-1523-2012, 2012. 3358

Ice sheet modelling of the last interglacial period

A. Quiquet et al.

[Title Page](#)[Abstract](#)[Introduction](#)[Conclusions](#)[References](#)[Tables](#)[Figures](#)[◀](#)[▶](#)[◀](#)[▶](#)[Back](#)[Close](#)[Full Screen / Esc](#)[Printer-friendly Version](#)[Interactive Discussion](#)

- Quiquet, A., Punge, H. J., Ritz, C., Fettweis, X., Kageyama, M., Krinner, G., Salas y Mélia, D., and Sjolte, J.: Large sensitivity of a Greenland ice sheet model to atmospheric forcing fields, *The Cryosphere Discuss.*, 6, 1037–1083, doi:10.5194/tcd-6-1037-2012, 2012. 3349, 3354, 3360
- 5 Rasmussen, S. O., Andersen, K. K., Svensson, A. M., Steffensen, J. P., Vinther, B. M., Clausen, H. . B., Siggaard-Andersen, M., Johnsen, S. J., Larsen, L. B., Dahl-Jensen, D., Bigler, M., Röthlisberger, R., Fischer, H., Goto-Azuma, K., Hansson, M. E., and Ruth, U.: A new Greenland ice core chronology for the last glacial termination, *J. Geophys. Res. Atmos.*, 111, 06102, 10.1029/2005JD006079, 2006. 3355
- 10 Reeh, N.: Parameterization of melt rate and surface temperature on the Greenland Ice Sheet, *Polarforschung*, 59, 113–128, 1991. 3352, 3377
- Ritz, C., Fabre, A., and Letréguilly, A.: Sensitivity of a Greenland ice sheet model to ice flow and ablation parameters: consequences for the evolution through the last climatic cycle, *Clim. Dynam.*, 13, 11–23, doi:10.1007/s003820050149, 1997. 3350, 3377
- 15 Ritz, C., Rommelaere, V., and Dumas, C.: Modeling the evolution of Antarctic ice sheet over the last 420,000 years: Implications for altitude changes in the Vostok region, *J. Geophys. Res.*, 106, 31943–31964, 2001. 3349
- Robinson, A., Calov, R., and Ganopolski, A.: Greenland ice sheet model parameters constrained using simulations of the Eemian Interglacial, *Clim. Past*, 7, 381–396, doi:10.5194/cp-7-381-2011, 2011. 3347, 3368
- 20 Salas-Mélia, D., Chauvin, F., Déqué, M., Douville, H., Gueremy, J. F., Marquet, P., Planton, S., Royer, J. F., and Tyteca, S.: Description and validation of the CNRM-CM3 global coupled model, CNRM working note, 103, 36 pp., 2005. 3354
- Shapiro, N. M. and Ritzwoller, M. H.: Inferring surface heat flux distributions guided by a global seismic model: particular application to Antarctica, *Earth Planet. Sci. Lett.*, 223, 213–224, doi:10.1016/j.epsl.2004.04.011, 2004. 3350, 3356, 3360
- 25 Tarasov, L. and Peltier, W. R.: Greenland glacial history and local geodynamic consequences, *Geophys. J. Int.*, 150, 198–229, doi:10.1046/j.1365-246X.2002.01702.x, 2002. 3352, 3369, 3377
- 30 Tarasov, L. and Peltier, W. R.: Greenland glacial history, borehole constraints, and Eemian extent, *J. Geophys. Res.*, 108, 2143, doi:10.1029/2001JB001731, 2003. 3347, 3350, 3368

Vernal, A. D. and Hillaire-Marcel, C.: Natural Variability of Greenland Climate, Vegetation, and Ice Volume During the Past Million Years, *Science*, 320, 1622–1625, doi:10.1126/science.1153929, 2008. 3347

5 Vezina, J., Jones, B., and Ford, D.: Sea-level highstands over the last 500,000 years; evidence from the Ironshore Formation on Grand Cayman, British West Indies, *J. Sediment. Res.*, 69, 317–327, 1999. 3346

Yoshimori, M. and Abe-Ouchi, A.: Sources of spread in multi-model projections of the Greenland ice-sheet surface mass balance, *J. Climate*, 25, 1157–1175, doi:10.1175/2011JCLI4011.1, 2012. 3350

Ice sheet modelling of the last interglacial period

A. Quiquet et al.

Title Page

Abstract

Introduction

Conclusions

References

Tables

Figures



Back

Close

Full Screen / Esc

Printer-friendly Version

Interactive Discussion



Ice sheet modelling of the last interglacial period

A. Quiquet et al.

Table 1. Previous estimates of maximal GIS melting contribution to global sea level rise during the LIG period.

| Study | SMB method | GIS melting (m of sea level equivalent) |
|-----------------------------|-----------------------------|---|
| Cuffey and Marshall (2000) | Index method | 4–5.5 |
| Tarasov and Peltier (2003) | Index method | 2.7–4.5 |
| Lhomme et al. (2005) | Index method | 3.5–4.5 |
| Otto-Bliesner et al. (2006) | Unidirectional GCM coupling | 2.2–3.4 |
| Robinson et al. (2011) | Energy-moisture coupling | 3.7–4.4 |
| This study | Index method | 0.7–1.5 |

Title Page

Abstract

Introduction

Conclusions

References

Tables

Figures

◀

▶

◀

▶

Back

Close

Full Screen / Esc

Printer-friendly Version

Interactive Discussion



Ice sheet modelling of the last interglacial period

A. Quiquet et al.

Table 2. Model parameters used in the GRISLI model for this study.

| Variable | Identifier name | Value |
|---|-----------------------------------|--|
| Basal drag coefficient | β | $1500 \text{ m yr}^{-1} \text{ Pa}^{-1}$ |
| SIA enhancement factor, Glen | E_3^{SIA} | 4.5 |
| SIA enhancement factor, linear | E_1^{SIA} | 1 |
| SSA enhancement factor, Glen | E_3^{SSA} | 0.6 |
| SSA enhancement factor, linear | E_1^{SSA} | 1 |
| Transition temperature of deformation, Glen | T_3^{trans} | -6.5°C |
| Activation energy below transition, Glen | Q_3^{cold} | $7.820 \cdot 10^4 \text{ J mol}^{-1}$ |
| Activation energy above transition, Glen | Q_3^{warm} | $9.545 \cdot 10^4 \text{ J mol}^{-1}$ |
| Transition temperature of deformation, linear | T_1^{trans} | -10°C |
| Activation energy below transition, linear | Q_1^{cold} | $4.0 \cdot 10^4 \text{ J mol}^{-1}$ |
| Activation energy above transition, linear | Q_1^{warm} | $6.0 \cdot 10^4 \text{ J mol}^{-1}$ |
| Topographic lapse rate, July | l_{rjuly} | $5.426^\circ\text{C km}^{-1}$ |
| Topographic lapse rate, annual | l_{rann} | $6.309^\circ\text{C km}^{-1}$ |
| Precipitation ratio parameter | γ | 0.11°C |
| PDD standard deviation of daily temperature | σ | 5.0°C |
| PDD snow and ice ablation coefficient | $C_{\text{snow}}, C_{\text{ice}}$ | Tarasov and Peltier (2002) |
| Isotopic slope for paleo-temperature | α' | $0.35\% \cdot ^\circ\text{C}^{-1}$ |

Title Page

Abstract

Introduction

Conclusions

References

Tables

Figures

◀

▶

◀

▶

Back

Close

Full Screen / Esc

Printer-friendly Version

Interactive Discussion



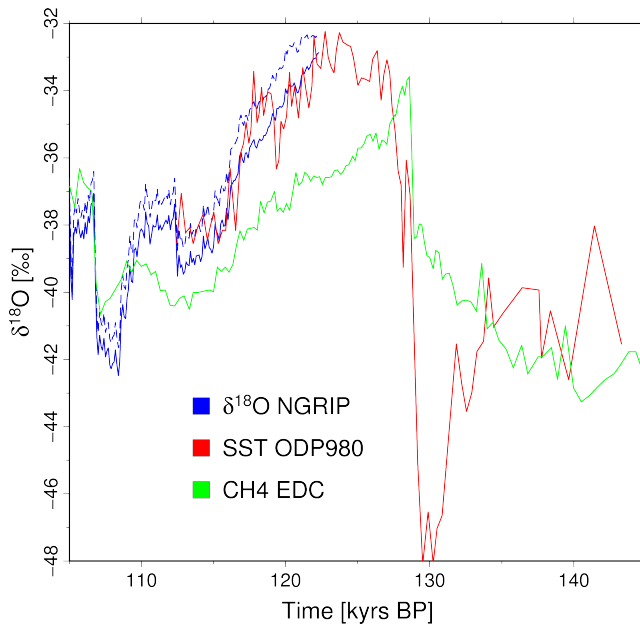


Fig. 1. Comparison between the 3 proxies used to generate the composite index around the LIG period. Blue: $\delta^{18}\text{O}$ at North GRIP. The plain line represents the direct measurement and the dashed line represents the value after the surface elevation changes correction. Red: SST reconstruction using ODP980 marine core, after scaling on the $\delta^{18}\text{O}$ record, corrected from elevation changes. Green: Methane concentration measured along the EPICA-DOME C ice core in Antarctica, after scaling on the $\delta^{18}\text{O}$ record, corrected from elevation changes. SST presents an important minimum at 130 ka BP, and transitions between methane to SST were done at 128.6 ka BP and 134 ka BP, both producing the same LIG retreat.

Ice sheet modelling of the last interglacial period

A. Quiquet et al.

Title Page

Abstract

Introduction

Conclusions

References

Tables

Figures



Back

Close

Full Screen / Esc

Printer-friendly Version

Interactive Discussion



Ice sheet modelling of the last interglacial period

A. Quiquet et al.

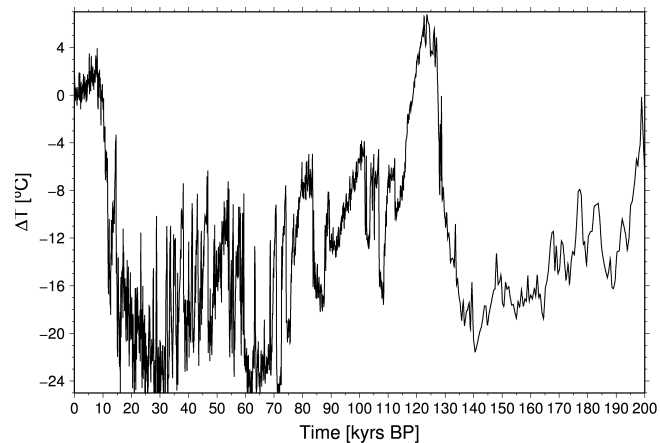


Fig. 2. Multi-proxy index used in this study. A warming greater than $+5^{\circ}\text{C}$ is prescribed during the LIG.

[Title Page](#)[Abstract](#)[Introduction](#)[Conclusions](#)[References](#)[Tables](#)[Figures](#)[◀](#)[▶](#)[◀](#)[▶](#)[Back](#)[Close](#)[Full Screen / Esc](#)[Printer-friendly Version](#)[Interactive Discussion](#)

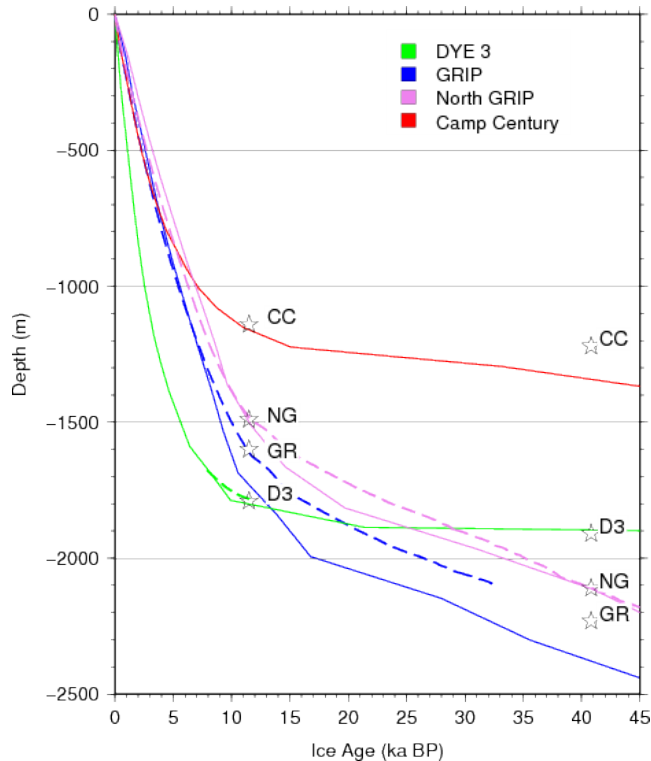


Fig. 3. Simulated age-depth relationship after calibration (plain line) and GICC05 (dashed lines) for four deep ice cores. The common GICC05 timescale is mainly available for GRIP and North GRIP for the long record, and for Dye 3 for the early Holocene. The stars represent the approximate depths of Younger Dryas (approx. 11.5 ka BP) and Laschamp event (approx. 40.8 ka BP). We mainly improve on the North GRIP dating with our calibration, as this record is used both as a forcing and as a constraint.

Ice sheet modelling of the last interglacial period

A. Quiquet et al.

Title Page

Abstract

Introduction

Conclusions

References

Tables

Figures

◀

▶

◀

▶

Back

Close

Full Screen / Esc

Printer-friendly Version

Interactive Discussion



Ice sheet modelling of the last interglacial period

A. Quiquet et al.

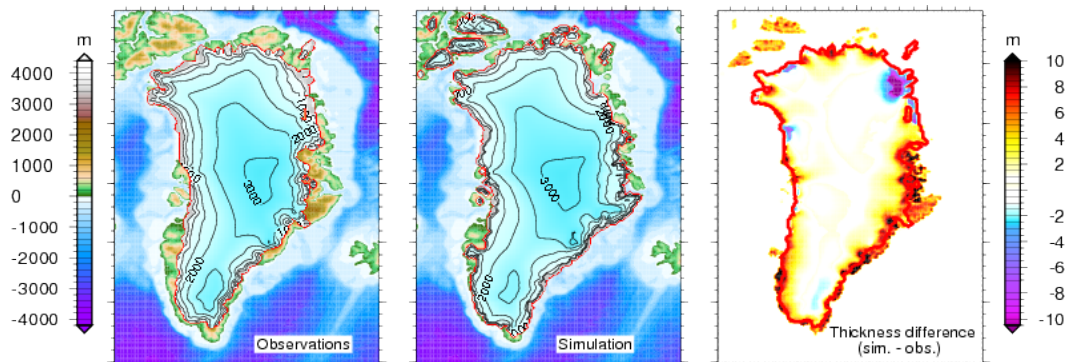


Fig. 4. Present day GIS geometry in the observations (Bamber et al., 2001) and simulated after a transient run with free surface evolution and with calibrated parameters. Ice thickness differences between simulation and observation are represented. The simulated present day ice sheet is generally too thick at the margins except in the northeastern region. The bedrock is far below sea level in this area, and the current ISM does not maintain this fjord englaciated. After calibration, the resulting simulated ice sheet presents a +0.8 m of sea level equivalent compared with observations.

[Title Page](#)[Abstract](#)[Introduction](#)[Conclusions](#)[References](#)[Tables](#)[Figures](#)[◀](#)[▶](#)[◀](#)[▶](#)[Back](#)[Close](#)[Full Screen / Esc](#)[Printer-friendly Version](#)[Interactive Discussion](#)

Ice sheet modelling of the last interglacial period

A. Quiquet et al.

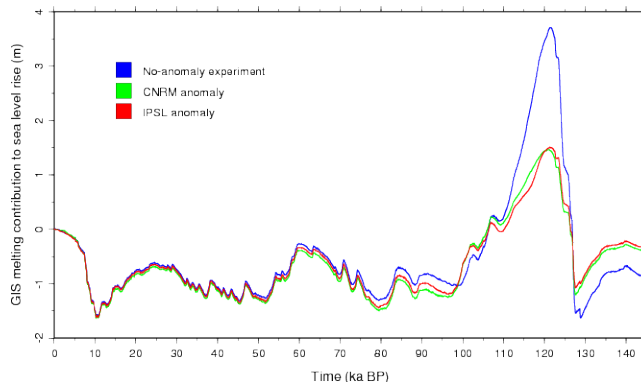


Fig. 5. Simulated Greenland melting contribution to global sea level rise. For the 0–100 ka BP the atmospheric forcings are the same in the three experiments, resulting in a very similar volume evolution. The plotted sea level rise contribution corresponds to the volume difference with the simulated present day volume in each experiment.

[Title Page](#)[Abstract](#)[Introduction](#)[Conclusions](#)[References](#)[Tables](#)[Figures](#)[⏪](#)[⏩](#)[◀](#)[▶](#)[Back](#)[Close](#)[Full Screen / Esc](#)[Printer-friendly Version](#)[Interactive Discussion](#)

Ice sheet modelling of the last interglacial period

A. Quiquet et al.

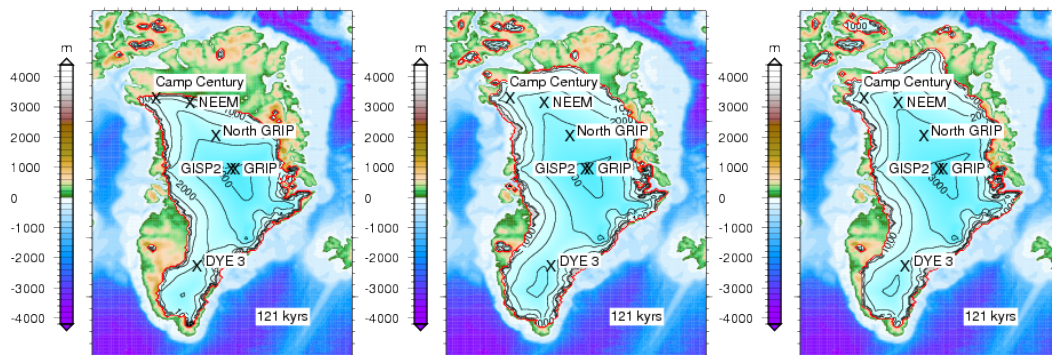


Fig. 6. Simulated GIS at 121 kyrs for: **(A)** No-anomaly experiment; **(B)** CNRM anomaly experiment; and **(C)** IPSL anomaly experiment. Deep ice cores are located on the map. Contour spacing is 500 m. The ice sheet margin is represented by the red contour.

[Title Page](#)[Abstract](#)[Introduction](#)[Conclusions](#)[References](#)[Tables](#)[Figures](#)[◀](#)[▶](#)[◀](#)[▶](#)[Back](#)[Close](#)[Full Screen / Esc](#)[Printer-friendly Version](#)[Interactive Discussion](#)

Ice sheet modelling of the last interglacial period

A. Quiquet et al.

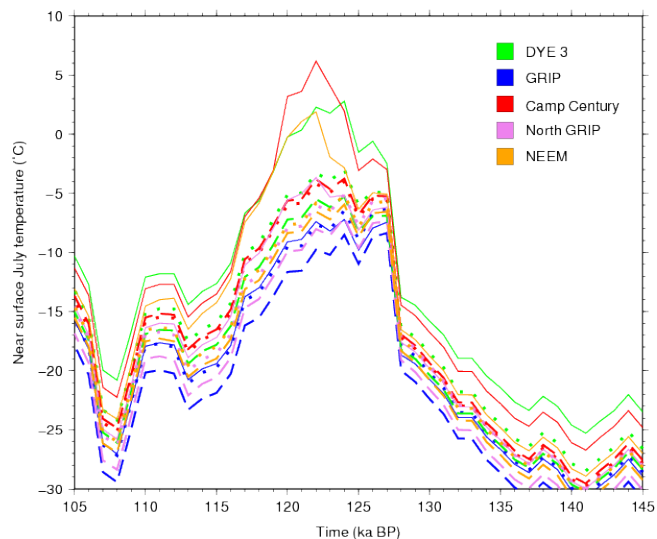


Fig. 7. July temperature evolution during the LIG at the deep ice core sites. Plain line: no-anomaly experiment; Dashed line: CNRM anomaly; dotted line: IPSL anomaly. Anomaly experiments always suggest lower values for July temperature. Melt may potentially occur at Dye 3, Camp Century and NEEM sites, even in the anomaly method.

Title Page

Abstract

Introduction

Conclusions

References

Tables

Figures

◀

▶

◀

▶

Back

Close

Full Screen / Esc

Printer-friendly Version

Interactive Discussion



Ice sheet modelling of the last interglacial period

A. Quiquet et al.

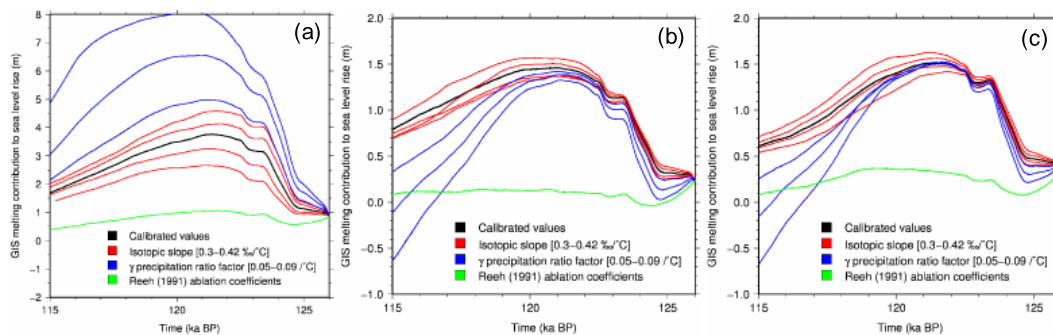


Fig. 8. Sensitivity of simulated GIS melting contribution to sea level rise during the LIG period to: isotopic slope which governs prescribed temperature anomaly amplitude, ranging from $0.30\text{‰}\text{°C}^{-1}$ (lower than calibrated value and corresponding to higher values of temperature anomalies) to $0.42\text{‰}\text{°C}^{-1}$ (higher than calibrated value and corresponding to lower values of temperature anomalies); precipitation ratio γ ranging from 0.05°C to 0.09°C , values lower than the calibrated one, which corresponds more to what is found in literature; the use of Reeh (1991) ablation coefficients rather than Tarasov and Peltier (2002) ones. **(a)**: no-anomaly experiment; **(b)**: CNRM anomaly; **(c)**: IPSL anomaly. The scales of volume variation is changed from **(a)** to **(b)** and **(c)**. The two experiments with GCM snapshots seems to be relatively robust to the choice of parameters. The experiment presenting the greatest retreat is the most sensitive one. Note that we cannot produce a realistic present day ice sheet with the original Reeh (1991) ablation coefficients, as already mentioned in Ritz et al. (1997).

Title Page

Abstract

Introduction

Conclusions

References

Tables

Figures

◀

▶

◀

▶

Back

Close

Full Screen / Esc

Printer-friendly Version

Interactive Discussion

